

# Metallurgical Method of Determining Heat Transfer Coefficient in Simulations of Twin-Roll Casting

Min-Seok Kim <sup>1,\*</sup> and Jiwon Kim <sup>2</sup><sup>1</sup> Department of Materials Science and Engineering, Gachon University, Seongnam-si 13120, Republic of Korea<sup>2</sup> Materials Science and Chemical Engineering Center, Institute for Advanced Engineering, Yongin-si 17180, Republic of Korea; jkim@iae.re.kr

\* Correspondence: mskim1205@gachon.ac.kr; Tel.: +82-031-750-5286

**Abstract:** We herein suggest a metallurgical method using pure aluminum with no freezing temperature range to derive appropriate roll/melt interfacial heat transfer coefficients in simulation of twin-roll casting process. This method is inspired by the concept that the position of the kiss points where two solidifying shells encounter and the roll nip coincides under the condition where the roll load becomes zero as the roll rotation speed decreases. The conditions where the roll load becomes zero under various melt supply temperature conditions in the actual TRC process are found experimentally. These conditions are then applied to simulation models to derive heat transfer coefficient values. When comparing these values with those derived previously from the empirical relation for roll rotation speed and heat transfer coefficient, the conclusion is drawn that the deviation was reasonably low, around 10%.

**Keywords:** twin-roll casting; simulation; heat transfer coefficient; pure aluminum

## 1. Introduction

Recently, in the aluminum sheet industry, the twin-roll casting (TRC) process has gained significant attention due to its economic advantages and high potential in future advanced alloy products [1]. For decades, the TRC process has been primarily used for the production of aluminum sheets, focusing on alloys such as 1xxx series, 3xxx, and 8xxx series [2–6]. However, in recent times, there has been active research and development on the manufacturing of high-alloy Al alloys, particularly for the production of sheets used in transportation equipment [7,8]. For high-alloy Al, such as the 5xxx series and 6xxx series, manufacturing is particularly challenging during continuous casting due to the wide freezing temperature range of the alloys [9–12]. This makes the process susceptible to surface inverse segregation and vulnerable to central segregation, posing significant difficulties in production [13–19].

An essential technology for overcoming these challenges is solidification analysis through simulation of the TRC process. For effective simulation of the TRC process, appropriate boundary conditions are fundamentally required [20]. In particular, achieving accurate predictions of solidification behavior during continuous casting necessitates a careful consideration of the heat transfer coefficients at the interface between the rotating rolls and the molten metal [21]. Numerous researchers have made considerable efforts to derive these heat transfer coefficients [7,20–23]. For basic simulations, it is common to use arbitrary heat transfer coefficients with constant values [22]. Deriving heat transfer coefficients through temperature measurements near the roll surface using heat flux tends to be more reliable for obtaining accurate values [23]. There are cases where thermocouples are directly inserted between the solidifying shells during the vertical-type high-speed twin-roll casting process to deduce heat transfer coefficients [21]. In this case, since direct temperature measurements are conducted, a certain level of reliable heat transfer coefficient



**Citation:** Kim, M.-S.; Kim, J. Metallurgical Method of Determining Heat Transfer Coefficient in Simulations of Twin-Roll Casting. *Metals* **2024**, *14*, 358. <https://doi.org/10.3390/met14030358>

Academic Editors: Noé Cheung and Menachem Bamberger

Received: 21 February 2024

Revised: 16 March 2024

Accepted: 17 March 2024

Published: 20 March 2024



**Copyright:** © 2024 by the authors. Licensee MDPI, Basel, Switzerland. This article is an open access article distributed under the terms and conditions of the Creative Commons Attribution (CC BY) license (<https://creativecommons.org/licenses/by/4.0/>).

values can be obtained. However, for high-speed TRC processes, which differ from conventional horizontal-type low-speed TRC processes in terms of strip manufacturing conditions, validation is necessary to apply existing empirical equations to low-speed processes. Additionally, in the case of the horizontal-type twin-roll casting process, the condition of the continuously rotating rolls and the extremely narrow space where solidification occurs in a very short time make experimental setups challenging and experimentation is highly difficult.

As shown in Figure 1, the twin-roll casting process fundamentally involves supplying molten metal between two rotating rolls. Two growing solid shells, formed on the rotating rolls, meet at a specific point (i.e., kiss point), joining to form a single strip. During this process, the strip, comprising two overlapping solid shells, expands the roll gap, subjecting the strip to some load from the rolls. The roll load applied at this point depends on the location of the kiss point. If the kiss point is formed before the roll nip, the sheet thickness is greater than the initial roll gap, resulting in a roll load on the sheet. Conversely, if the kiss point is formed after the roll nip, the combined thickness of the solidifying shells is less than the initial roll gap, and no roll load is applied. While the position of the kiss point indeed influences the load on the rolls, defining the kiss point is difficult for most alloys since the solidifying shells undergo mush-type solidification in a semi-solid state. On the other hand, for pure metals with freezing temperature ranges close to zero, such as pure aluminum, the solidification shells form in a planar solid front state, making the location of the kiss point relatively distinct. Leveraging this characteristic, this study aims to indirectly deduce the kiss point by examining the variations in roll load in the twin-roll casting process using pure aluminum. Additionally, this study seeks to develop a relatively straightforward metallurgical method for deriving appropriate heat transfer coefficients based on this information.

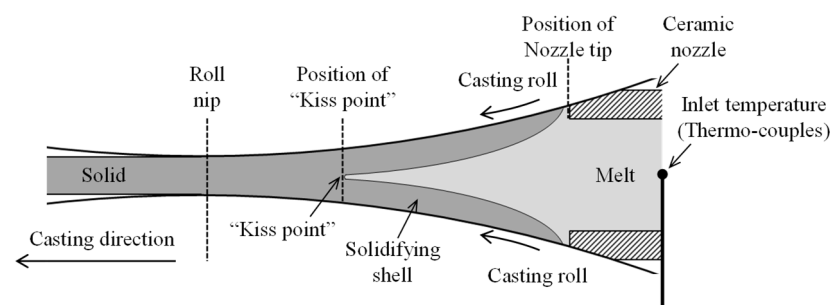


**Figure 1.** Schematic diagram of twin-roll casting process.

## 2. Materials and Methods

### 2.1. Strip Fabrication Using Twin-Roll Casting

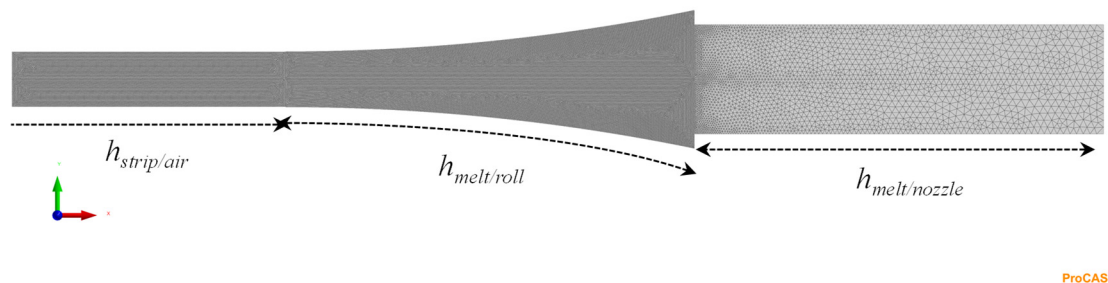
Commercially pure Al (Al-0.04Si-0.03Fe, in wt%) was melted in an electric furnace, and degassing was conducted using Ar gas for 10 min prior to casting. Horizontal-type twin-roll casters were used for strip fabrication. The caster consists of two rolls with a diameter of 300 mm each. The roll surfaces were polished with #1000 sandpapers before TRC to maintain consistent cooling capability. The set-back distance and the initial roll gap were set to be 30 mm and 4 mm, respectively, and 100 mm wide sheets were produced. Twin-roll casting was conducted under two molten metal supply temperature conditions (730 °C, 760 °C). To accurately determine the temperature at which the molten metal makes contact with the roll surface as it passes through the nozzle, thermocouples were installed about 50 mm away from the nozzle tip to measure the inlet temperature, as shown in Figure 1. The temperature measurement results were 677 °C and 707 °C, indicating temperatures approximately 60 °C lower than the initial molten metal supply temperature. To vary the roll load during continuous casting, the roll rotation speed was continuously adjusted in the range of 5 to 2 m/min. For the cast strip, longitudinal cross-sectioned samples were

mounted in epoxy resin prior to mechanical polishing. The samples were anodized at 40 V in a 3.3% solution of  $\text{HBF}_4$  in distilled water to reveal their grain structures.

## 2.2. Simulation Model for Twin-Roll Casting Process

Heat transfer simulations were conducted to investigate the temperature distribution and solidification behavior during the TRC. The model geometry, calculated thermo-physical data of the pure Al, and the boundary conditions are given in Table 1. Gradual mesh size was applied to the surface of the model by considering the importance of each part. The mesh size for the solidification and strip parts was set to 0.2 mm. The thermo-physical data for pure aluminum were calculated using the PanAl2021 database, and simulations were performed using the commercial software ProCAST 2021. The simulation calculations were performed under Scheil cooling conditions, considering a rapid average cooling rate of over  $100\text{ }^\circ\text{C/s}$ .

**Table 1.** Model geometry, thermo-physical properties and boundary conditions.



Casting alloy: Pure Al

Initial melt temperature:  $677\text{ }^\circ\text{C}$ ,  $707\text{ }^\circ\text{C}$

Liquidus temperature:  $660\text{ }^\circ\text{C}$

Solidus temperature:  $659\text{ }^\circ\text{C}$

Temperature ( $^\circ\text{C}$ )	Thermal Conductivity ( $\text{W/mK}$ )	Density ( $\text{kg/m}^3$ )	Enthalpy ( $\text{kJ/kg}$ )
403	174	2618	374
505	177	2593	486
659	179	2552	673
802	92	2350	1233

Interfacial heat transfer coefficient (HTC,  $h$ );  $h_{\text{melt/nozzle}}$ : adiabatic;  $h_{\text{strip/air}}$ :  $12\text{ W/m}^2\text{K}$ ;  $h_{\text{melt/roll}}$ : variable; Roll temperature:  $100\text{ }^\circ\text{C}$ ; Air temperature:  $25\text{ }^\circ\text{C}$ .

## 3. Results and Discussion

### 3.1. Influence of Roll Rotation Speed on Roll Load during TRC Process

Figure 2 shows the appearance and cross-sectional microstructure of pure Al strips manufactured through the TRC process. In Figure 2a, the surface of the as-cast strip illustrates the appearance formed by the rolling load in the conventional TRC process. The cross-sectional microstructure (Figure 2b) reveals the typical TRC strip structure, where initially formed columnar crystals were elongated by the rolling load during continuous casting. From this figure, it can be inferred that the rolling load was applied to the strip (solidifying shells), indicating that the kiss point, where two solidification shells met during continuous casting, formed prior to the roll nip. It is worth noting that in this experiment, careful attention was paid to maintaining a homogeneous surface condition in the strip width direction at each condition of roll speed to obtain a reliable roll load, which can be affected by the formation of an inhomogeneous solidification shell thickness in the width direction of the strip. Therefore, by gradually increasing the rolling speed during continuous casting using this process, if the thickness of the solidification shell is reduced, the rolling load applied to the strip becomes zero when the kiss point is formed at the roll

nip, under the condition where the solidification shell thickness and the initial roll gap are the same.

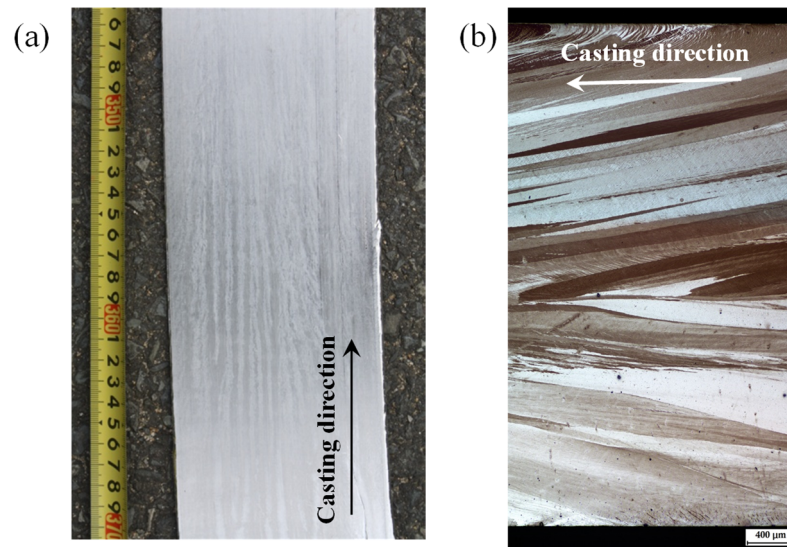


**Figure 2.** (a) Appearance of pure Al strip fabricated by TRC process, and (b) anodized grain structure of the longitudinal cross-section of the strip.

Figure 3 shows the variation in roll load on the TRC sheet under various roll rotation speeds and melt supply temperatures. It can be observed that as the roll rotation speed increases under each temperature condition, the thickness of the solidified shell decreases, leading to a decrease in roll load. The roll load decreases until it approaches zero at a certain speed condition. This indicates that a kiss point is formed at the roll nip, where the thickness of the two roll shells is equal to the initial roll gap. The experimental results indicate that under melt supply temperature conditions of 730 °C and 760 °C, roll loads approached zero at speeds of approximately 4.2 m/min and 3.1 m/min, respectively.

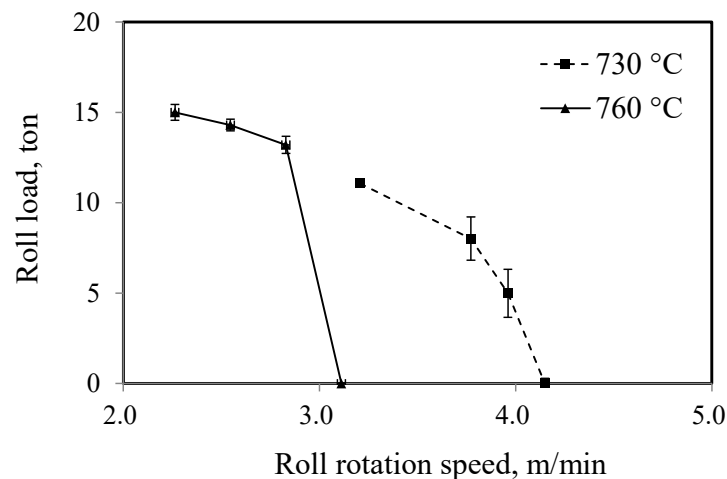


**Figure 3.** Variation in roll load under various roll rotation speeds and melt supply temperatures.

### 3.2. Influence of Heat Transfer Coefficient on Kiss Point in TRC Simulation

Simulation calculations were performed under roll rotation speed conditions of 4.2 m/min and 3.1 m/min, applying various melt/roll interfacial heat transfer coefficient (HTC) values. Figure 4 illustrates the solidification behavior under different HTC conditions. The simulation results show that as the melt/roll interfacial HTC decreases, the kiss point, where two solidified shells meet, moves toward the roll nip. As mentioned

above, experimentally derived conditions of 4.2 m/min and 3.1 m/min exhibit zero value in the roll load. It can be conjectured that in these two experimental conditions, during continuous casting, the kiss point lies at the roll nip. This is because the roll load is imposed as the two solidifying shells expand the roll gap and engage the strip. However, when the two solidifying shells meet at the roll nip, the thickness of the solidifying shells is equal to the initially set roll gap thickness, preventing further expansion of the roll gap, resulting in zero roll load. The derived casting speed conditions represent the onset of roll load reduction toward zero, suggesting that the kiss point is likely positioned at the roll nip at this point. From this perspective, simulation results yielded appropriate HTC values positioning the kiss point at the roll nip. Figure 5 depicts the variation in the position of the kiss point with changes in the HTC. The Y-axis represents the distance between the roll nip and the kiss point in the simulation results, with a negative Y-axis value indicating that the kiss point is forming beyond the roll nip. The appropriate values for the HTC were found to be 9700 W/m<sup>2</sup>K and 7600 W/m<sup>2</sup>K for the conditions of 4.2 m/min and 3.1 m/min, respectively, as also shown in Figure 4.

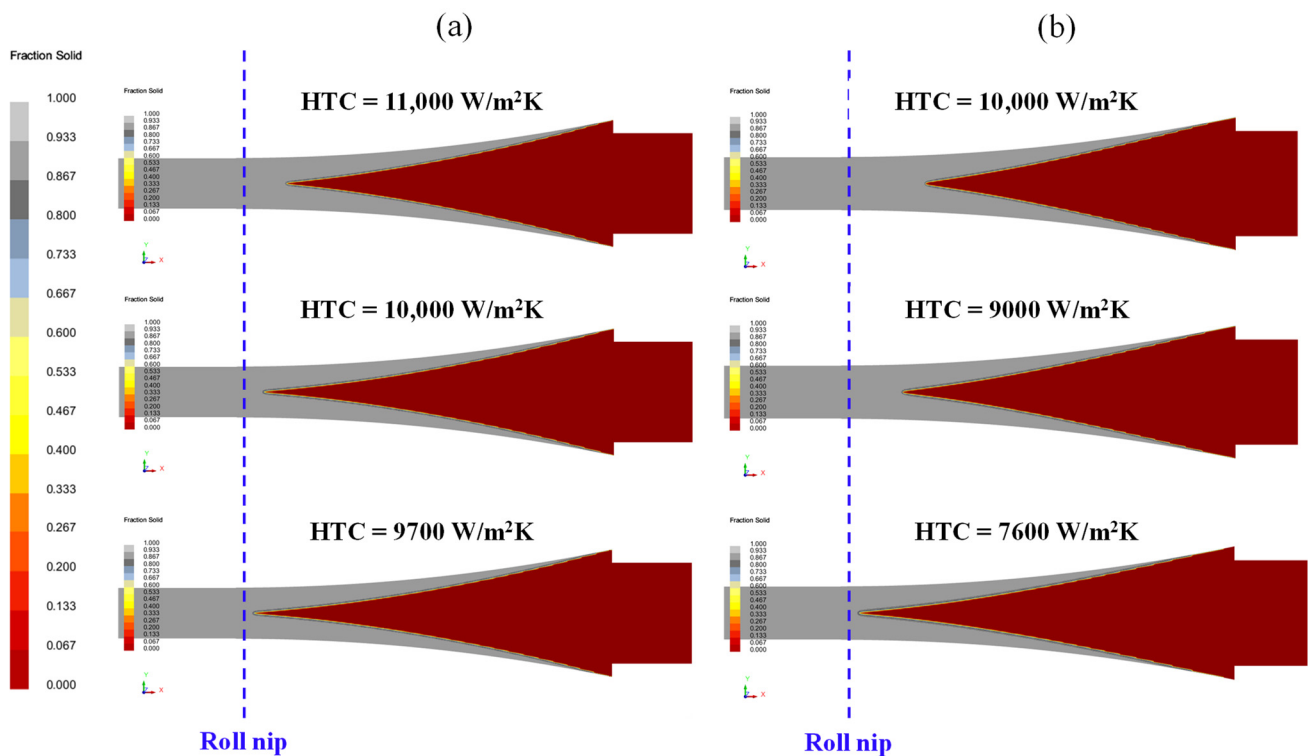


**Figure 4.** The influence of the roll/melt interfacial HTC on solidification behavior in TRC process, (a) 4.2 m/min and (b) 3.1 m/min.

### 3.3. Verification of the Derived HTC Values

In general, the twin roll casting process is not standardized and comes in various forms compared to the traditional direct-chill casting process. For instance, the melt supply and roll operating systems are categorized into vertical, horizontal, and tilted types [6]. The roll rotation speed also varies from the traditional low-speed range (approximately 0.5~2 m/min) to recently developed high-speed TRC processes, encompassing a broad speed range (approximately 20~100 m/min) [24,25]. In the case of TRC simulation models, the heat transfer coefficient between the molten metal and the rolls is a crucial factor for predicting solidification behavior. However, determining generalized HTCs for various TRC process conditions can be challenging. Therefore, a previous study derived the empirical relationships for the variation in HTC with roll rotation speed [21]:

$$h = 44.8v^{0.55} \quad (1)$$

where  $h$  is the roll/melt interfacial HTC ( $\text{kW}/\text{m}^2\text{K}$ ), and  $v$  is the roll rotation speed ( $\text{m}/\text{s}$ ). Using this empirical relationship, the appropriate heat transfer coefficient values for current roll rotation speeds of 4.2  $\text{m}/\text{min}$  and 3.1  $\text{m}/\text{min}$  are calculated to be approximately 10,300  $\text{W}/\text{m}^2\text{K}$  and 8800  $\text{W}/\text{m}^2\text{K}$ , respectively. These values represent approximately 6% and 16% errors compared to the values derived using the metallurgical method proposed in this study. From these results, it can be inferred that the metallurgically approached method for obtaining heat transfer coefficients is quite reasonable. Furthermore, it is evident that the empirical relationship for heat transfer coefficients obtained under high-speed TRC conditions is applicable not only in the high-speed range but also effectively extends to the low-speed range of 5  $\text{m}/\text{min}$  and below.

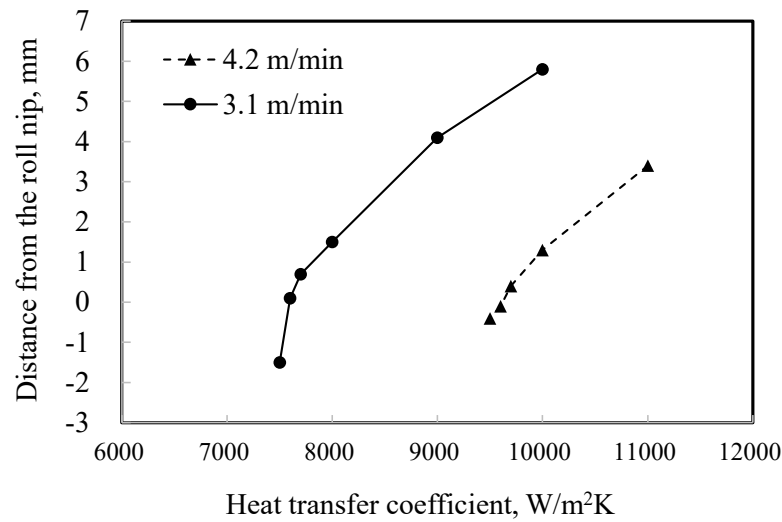


**Figure 5.** Relationship between the roll/melt interfacial HTC and the position of the kiss point (distance from the roll nip to the kiss point).

These results imply several important points. Firstly, in the conventional horizontal low-speed TRC process, the area where solidification occurs is very narrow, making direct temperature measurement very difficult during the continuous casting. Furthermore, solving the inverse heat transfer problem [23], which can be inferred from temperature measurements at the casting roll, is limited to specific equipment or casting conditions, making it difficult to generalize the results. The metallurgical method proposed in this study has the advantage of relatively low experimental complexity and applicability to any metal. Additionally, the results of this study demonstrate that empirical equation derived from high-speed TRC conditions can also be applied to low-speed TRC conditions. This indicates that this empirical equation can be practically useful for predicting the solidification behavior regardless of specific equipment conditions in the TRC process. However, since this empirical equation does not directly account for various process conditions such as casting alloys, roll surface conditions, and hydrostatic melt pressure, it may introduce an error of approximately 10%. Therefore, when applying this empirical equation to TRC simulation models, it is necessary to consider the factors that can cause such errors in order to predict the detailed solidification behavior of specific regions.

#### 4. Conclusions

The twin-roll casting process enables the direct manufacturing of aluminum strips from molten metal, making it considerably more economical and seemingly simpler compared to conventional direct-chill casting and hot-rolling processes. Despite these advantages, due to the need to control solidification behavior within a short timeframe, the TRC process is challenging. Therefore, recent research has extensively focused on studying solidification behavior and defect control through simulations. However, the TRC process presents

difficulties in predicting solidification behavior in simulation models, primarily due to various roll settings and a wide range of process speeds.

This study developed a metallurgical method using pure aluminum to derive appropriate heat transfer coefficient values. This method is inspired by the concept that, in the case of pure aluminum with no freezing temperature range, the position of the kiss points where two solidifying shells meet and the roll nip coincide under the condition where the roll load becomes zero as the roll rotation speed decreases. The conditions where the roll load becomes zero under various melt supply temperature conditions in the actual TRC process were found experimentally. These conditions were then applied to simulations to derive heat transfer coefficient values. When comparing these values with those derived previously from the empirical relationship for roll rotation speed and heat transfer coefficient in the high-speed TRC process, the conclusion was drawn that the deviation was reasonably low, around 10%. This result is considered highly significant in demonstrating that, even in the horizontal low-speed TRC process where the solidification region is very narrow, it is relatively straightforward to derive heat transfer coefficients despite the difficulty of actual temperature measurements. Furthermore, it indicates that the heat transfer coefficient equations derived from high-speed TRC conditions are applicable to the low-speed TRC processes as well.

**Author Contributions:** Conceptualization, M.-S.K.; methodology, M.-S.K.; validation, J.K.; formal analysis, M.-S.K.; investigation, M.-S.K.; resources, J.K.; data curation, M.-S.K.; writing—original draft preparation, M.-S.K.; writing—review and editing, J.K.; visualization, M.-S.K.; supervision, M.-S.K. and J.K.; project administration, M.-S.K. and J.K.; funding acquisition, M.-S.K. and J.K. All authors have read and agreed to the published version of the manuscript.

**Funding:** This work was supported by the Materials and Components Technology Development Program (No. 20017369) and the Technology Innovation Program (No. 20010638, No. 20016338) funded by the Ministry of Trade, Industry and Energy (MOTIE, Korea), Republic of Korea.

**Data Availability Statement:** The raw data supporting the conclusions of this article will be made available by the authors on request.

**Conflicts of Interest:** The authors declare no conflicts of interest.

## References

1. Cook, R.; Grocock, P.G.; Thomas, P.M.; Edmonds, D.V.; Hunt, J.D. Development of the twin-roll casting process. *J. Mater. Process. Technol.* **1995**, *55*, 76–84. [[CrossRef](#)]
2. Zhao, X.; Jin, T.; Ding, L.; Wan, B.; Lei, X.; Xu, C.; Zhang, C.; Jia, Z.; Liu, Q. The effect of combined cold rolling and homogenization on the microstructures and mechanical properties of twin-roll casted 8021 aluminum alloy. *J. Alloys Compd.* **2023**, *937*, 168385. [[CrossRef](#)]
3. Jin, T.; Xiao, H.; Ding, L.; Zhao, X.; Lei, X.; Wan, B.; Weng, Y.; Jia, Z.; Liu, Q. Effect of homogenization temperature on microstructural homogeneity and mechanical properties of twin-roll casted 8006 aluminum alloy. *Mater. Charact.* **2023**, *200*, 112857. [[CrossRef](#)]
4. Kumar, R.; Gupta, A.; Kumar, A.; Chuhan, R.N.; Khatirkar, R. Microstructure and texture development during deformation and recrystallisation in strip cast AA8011 aluminum alloy. *J. Alloys Compd.* **2018**, *742*, 369–382. [[CrossRef](#)]
5. Wang, W.X.; Zhang, J.X.; Wang, Z.J.; Liu, W.C. A comparative study of the transformation kinetics of recrystallization texture of CC and DC 3003 aluminum alloys. *Mater. Charact.* **2018**, *141*, 412–422. [[CrossRef](#)]
6. Birol, Y. Analysis of macro segregation in twin-roll cast aluminum strips via solidification curves. *J. Alloys Compd.* **2009**, *486*, 168–172. [[CrossRef](#)]
7. Barekar, N.S.; Dhindaw, B.K. Twin-roll casting of aluminum alloys—an overview. *Mater. Manuf. Proc.* **2014**, *29*, 651–661. [[CrossRef](#)]
8. Kumai, S. Role and Potential of Aluminium and Its Alloys for a Zero-Carbon Society. *Mater. Trans.* **2023**, *64*, 319–333. [[CrossRef](#)]
9. Jin, J.W.; Zhang, Z.J.; Li, R.H.; Li, Y.; Gong, B.S.; Hou, J.P.; Wang, H.W.; Zhou, X.H.; Purcek, G.; Zhang, Z.F. Mechanical properties of three typical aluminum alloy strips prepared by twin-roll casting. *J. Mater. Res. Technol.* **2024**, *28*, 500–511. [[CrossRef](#)]
10. Ymazaki, K.; Haga, T. High-Speed and Low-Load Twin-Roll Casting of Al-5%Mg Strip. *Metals* **2023**, *19*, 72. [[CrossRef](#)]
11. Wang, J.; Han, J.; Dou, R.; Chen, D.; Zhang, M.; Huang, H. Rationalizing Al-Mg, Al-Mg-Si, and multicomponent aluminum alloy design with segregation susceptibility predictions. *Mater. Today Commun.* **2020**, *25*, 101376. [[CrossRef](#)]
12. Kim, M.S.; Arai, Y.; Hori, Y.; Kumai, S. Formation of internal crack in high-speed twin-roll cast 6022 aluminum alloy strip. *Mater. Trans.* **2010**, *51*, 1854–1860. [[CrossRef](#)]

13. Wang, B.; Zhao, Q.; Qiu, F.; Jiang, Q. Effect of Mg and Si contents and TiC nanoparticles on the center segregation susceptibility of twin-roll cast Al-Mg-Si alloys. *J. Mater. Res. Technol.* **2023**, *25*, 411–419. [[CrossRef](#)]
14. Zhang, J.; Yuan, H.; Zhang, T.; Fu, J.; Xu, G.; Li, Y. A novel approach to improve the macrosegregation defect and mechanical properties of Al-Mg-Mn aluminum alloys during twin-roll continuous casting. *J. Mater. Res. Technol.* **2023**, *22*, 3170–3179. [[CrossRef](#)]
15. Wu, X.; Guan, Z.; Yang, Z.; Wang, W.; Qiu, F.; Wang, H. Effect of Cu content on central-segregation composition and mechanical properties of Al-Mg-Si alloys produced by twin-roll casting. *Mater. Sci. Eng. A* **2023**, *869*, 144782. [[CrossRef](#)]
16. Lu, B.; Li, Y.; Yu, W.; Wang, H.; Wang, Y.; Wang, Z.; Xu, G. Strength and ductility enhancement of twin-roll cast Al-Zn-Mg-Cu alloys with high solidification intervals through a synergistic segregation-controlling strategy. *Mater. Sci. Eng. A* **2023**, *142*, 225–239. [[CrossRef](#)]
17. Kim, M.S.; Kim, S.H.; Kim, H.W. Deformation-induced center segregation in twin-roll cast high-Mg Al-Mg strips. *Scripta Mater.* **2018**, *152*, 69–73. [[CrossRef](#)]
18. Yu, W.; Li, Y.; Jiang, T.; Wang, Y.; Zhang, B.; Li, X.; Wang, Z.; Xu, G.; Li, J. Solute inverse segregation behavior in twin roll casting of an Al-Cu alloy. *Scripta Mater.* **2022**, *213*, 114592. [[CrossRef](#)]
19. Yun, M.; Lokyer, S.; Hunt, J.D. Twin roll casting of aluminum alloys. *Mater. Sci. Eng. A* **2000**, *280*, 69–73. [[CrossRef](#)]
20. Saxena, A.; Sahai, Y. Modeling of fluid flow and heat transfer in twin-roll casting of aluminum alloys. *Mater. Trans.* **2002**, *43*, 206–213. [[CrossRef](#)]
21. Kim, M.S.; Kim, H.W.; Kumai, S. Direct temperature measurement of Al-2mass%Si alloy strips during high-speed twin-roll casting and its application in determining melt/roll heat transfer coefficient for simulation. *Mater. Trans.* **2017**, *58*, 967–970. [[CrossRef](#)]
22. Liu, X.; Song, J.; Wang, X.; Li, Z.; Zhang, S.; Jia, W.; Wang, C.; Wang, H. Prediction on the solidification behavior of AA6005 aluminum alloys produced by inclined twin-roll casting: A finite element analysis. *J. Mater. Res. Technol.* **2024**, *29*, 2405–2413. [[CrossRef](#)]
23. Wang, D.; Zhou, C.; Xu, G.; Huaiyuan, A. Heat transfer behavior of top side-pouring twin-roll casting. *J. Mater. Proc. Tech.* **2014**, *214*, 1275–1284. [[CrossRef](#)]
24. Haga, T.; Takahashi, K.; Ikawa, M.; Watari, H. A vertical-type twin roll caster for aluminum alloy strips. *J. Mater. Proc. Tech.* **2003**, *140*, 610–615. [[CrossRef](#)]
25. Haga, T.; Takahashi, K.; Ikawa, M.; Watari, H. Twin-roll casting of aluminum alloy strips. *J. Mater. Proc. Tech.* **2004**, *153–154*, 42–47. [[CrossRef](#)]

**Disclaimer/Publisher’s Note:** The statements, opinions and data contained in all publications are solely those of the individual author(s) and contributor(s) and not of MDPI and/or the editor(s). MDPI and/or the editor(s) disclaim responsibility for any injury to people or property resulting from any ideas, methods, instructions or products referred to in the content.